# Solutions to the Discrete Airy Equation: Application to Parabolic Equation Calculations

Matthias Ehrhardt [a,*,1] and Ronald E. Mickens [b,2]

[a] *Institut für Mathematik, Technische Universität Berlin, Straße des 17. Juni 136, D–10623 Berlin, Germany*

[b] *Department of Physics, Clark Atlanta University, Atlanta, GA 30314, USA*

**Abstract**

In the case of the equidistant discretization of the Airy differential equation ("discrete Airy equation") the exact solution can be found explicitly. This fact is used to derive a discrete transparent boundary condition (TBC) for a Schrödinger–type equation with linear varying potential, which can be used in "parabolic equation" simulations in (underwater) acoustics and for radar propagation in the troposphere. We propose different strategies for the discrete TBC and show an efficient implementation. Finally a stability proof for the resulting scheme is given. A numerical example in the application to underwater acoustics shows the superiority of the new discrete TBC.

*Key words:* discrete Airy equation, discrete transparent boundary condition, difference equation, Schrödinger–type equation, parabolic equation prediction
*PACS:* 02.70.Bf, 43.30.+m, 92.10.Vz

* Corresponding author.
*Email addresses:* `ehrhardt@math.tu-berlin.de` (Matthias Ehrhardt), `rohrs@math.gatech.edu` (Ronald E. Mickens).
*URL:* `http://www.math.tu-berlin.de/~ehrhardt/` (Matthias Ehrhardt).

[1] Supported by the DFG Research Center "Mathematics for key technologies" (FZT 86) in Berlin.
[2] Research supported by DOE and the MBRS–SCORE Program.

## 1 Introduction

In this work we consider the *Airy differential equation*

$$\frac{\mathrm{d}^2 y}{\mathrm{d}x^2} - xy = 0. \tag{1}$$

The solutions of this second-order differential equation (1) are called *Airy functions* and can be expressed in terms of *Bessel functions of imaginary argument* of order $\nu = \pm\frac{1}{3}$. They play an important role in the theory of asymptotic expansions of various special functions and have a wide range of applications in mathematical physics.

The two linearly independent solutions of (1), the *Airy functions of the first and second kind* $\mathrm{Ai}(x)$, $\mathrm{Bi}(x)$, respectively have the following asymptotic representation for large $|x|$ [10]:

$$\mathrm{Ai}(x) = \frac{1}{2\sqrt{\pi}}\, x^{-1/4}\, e^{-2/3x^{3/2}}[1 + \mathrm{O}(|x|^{-3/2})], \tag{2a}$$

$$\mathrm{Bi}(x) = \frac{1}{\sqrt{\pi}}\, x^{-1/4}\, e^{2/3x^{3/2}}[1 + \mathrm{O}(|x|^{-3/2})]. \tag{2b}$$

To solve the Airy equation (1) numerically we introduce the uniform grid points $x_m = m\Delta x$, $y_m \simeq y(x_m)$, and consider the *standard discretization*:

$$\frac{y_{m+1} - 2\, y_m + y_{m-1}}{(\Delta x)^2} - x_m y_m = 0, \tag{3}$$

which can be rewritten as the second-order difference equation

$$y_{m+1} - 2\, y_m + y_{m-1} - c\, m\, y_m = 0, \quad c = (\Delta x)^3. \tag{4}$$

In [15] Mickens derived the following asymptotic behaviour of the two linearly independent discrete solutions to (4) with $c = 1$:

$$y_m^{(1)} = \left[\frac{m^{7/2}\, e^m}{m^m}\right]\left\{1 - \frac{85}{12m} + \mathrm{O}\left(\frac{1}{m^2}\right)\right\}, \tag{5a}$$

$$y_m^{(2)} = \left[\frac{m^m\, e^{-m}}{m^{9/2}}\right]\left\{1 + \frac{133}{12m} + \mathrm{O}\left(\frac{1}{m^2}\right)\right\}. \tag{5b}$$

It can easily be seen that the solutions to this discretization (4) do not have the same asymptotic properties as the solutions of (1) which motivated the construction of a *nonstandard discretization scheme* (cf. [15], [16]).

This paper is organized as follows: first we discuss a generalization of the the *discrete Airy equation* (4) and show how to find exact and asymptotic solutions. Afterwards we present an application to a problem arising in "parabolic equation" calculations in (underwater) acoustics and radar propagation in the troposphere: we construct a so-called *discrete transparent boundary condition* (DTBC) for a Schrödinger equation with a linear potential term, discuss different approaches and present an efficient implementation by the sum-of-exponentials ansatz. Afterwards we analyze the stability of the resulting numerical scheme. In this case the Laplace transformed Schrödinger equation can be viewed as a general Airy equation. Discrete transparent boundary conditions for a Schrödinger equation with constant potential were derived in [1] and a generalization to a problem arising in (underwater) acoustics was presented in [2]. The construction of DTBC to the nonstandard discretization scheme and to wide-angle parabolic equations will be a topic of future work. Finally we illustrate the results with a numerical example from underwater acoustics.

## 2 Exact and asymptotic solutions to the discrete Airy equation

In this section we consider the *discrete Airy equation* in the more general form

$$y_{m+1} - 2\,y_m + y_{m-1} - (d + c\,m)\,y_m = 0, \quad c, d \in \mathbb{C}. \tag{6}$$

and show how to determine asymptotic solutions. This is a nontrivial task since equation (6) is not of Poincaré type. Afterwards we will demonstrate how to obtain an explicit solution to (6).

**The asymptotic solution**. Since the classic theorems of Poincaré and Perron cannot be applied to (6) it is not straight forward to obtain information about the asymptotic behaviour of the solutions to this equation. One possible ansatz is the one of Batchelder [5] given in [15] (see (5) in the case $c = 1$, $d = 0$). Here we want to apply the approach of Wong and Li [21] to obtain asymptotic solutions to the second–order difference equation

$$y_{m+2} + m^p\,a(m)\,y_{m+1} + m^q\,b(m)\,y_m = 0, \tag{7}$$

where $p$, $q$ are integers and $a(m)$ and $b(m)$ have power expansions of the form

$$a(m) = \sum_{s=0}^{\infty} \frac{a_s}{m^s}, \qquad b(m) = \sum_{s=0}^{\infty} \frac{a_s}{m^s}, \tag{8}$$

with nonzero leading coefficients: $a_0 \neq 0$, $b_0 \neq 0$. We increase the index of (6) by one to put it in the form of (7) and make the following identifications:

$$\begin{aligned} &a_0 = -c, \quad a_1 = -(2 + c + d), \quad a_s = 0, \; s \geq 2, \\ &b_0 = 1, \quad b_s = 0, \; s \geq 1, \quad p = 1, \quad q = 0. \end{aligned}$$

Then the two formal series solutions (cf. [21]) are given by

$$y_m^{(1)} = \frac{c^{-m}}{(m-2)!}\, m^{-2-(2+d)/c} \sum_{s=0}^{\infty} \frac{c_s^{(1)}}{m^s}, \tag{9a}$$

$$y_m^{(2)} = (m-2)!\, c^m\, m^{1+(2+d)/c} \sum_{s=0}^{\infty} \frac{c_s^{(2)}}{m^s}. \tag{9b}$$

To determine the values of the coefficients $c_1^{(1)}$, $c_2^{(1)}$, $c_3^{(1)}, \ldots$ we substitute the decaying solution $y_m^{(1)}$ in (7):

$$\frac{1}{cm}\Big(\frac{m+1}{m+2}\Big)^{\theta} \sum_{s=0}^{\infty} \frac{c_s^{(1)}}{(m+2)^s} + c(m-1)\Big(\frac{m+1}{m}\Big)^{\theta} \sum_{s=0}^{\infty} \frac{c_s^{(1)}}{m^s} \\ = \Big(c(\theta-1)+cm\Big) \sum_{s=0}^{\infty} \frac{c_s^{(1)}}{(m+1)^s}, \tag{10}$$

with $\theta = 2 + (2+d)/c$. We now obtain after an Taylor expansion in $1/m$ and setting all the linearly independent terms equal to zero, by a lengthy but elementary calculation, the results:

$$c_1^{(1)} = -c_0^{(1)}\Big[c^{-2} - \theta + \frac{\theta}{2}(\theta-1)\Big], \tag{11a}$$

$$c_2^{(1)} = \frac{c_0^{(1)}}{2}\Big[\theta c^{-2} + \frac{\theta}{2}(\theta-1) - \frac{\theta}{6}(\theta-1)(\theta-2)\Big] - \frac{c_1^{(1)}}{2}\Big[c^{-2} - 2 + \frac{\theta}{2}(\theta-1)\Big], \tag{11b}$$

$$c_3^{(1)} = -\frac{c_0^{(1)}}{3}\Big[\Big(2\theta + \frac{\theta}{2}(\theta-1)\Big)c^{-2} - \frac{\theta}{6}(\theta-1)(\theta-2) - \frac{\theta}{24}(\theta-1)(\theta-2)(\theta-3)\Big] \\ + \frac{c_1^{(1)}}{3}\Big[(2+\theta)c^{-2} - 2 + \theta + \frac{\theta}{2}(\theta-1) - \frac{\theta}{6}(\theta-1)(\theta-2)\Big] \\ - \frac{c_2^{(1)}}{3}\Big[c^{-2} - 5 + \theta + \frac{\theta}{2}(\theta-1)\Big], \tag{11c}$$

etc..

Similarly we obtain for the increasing solution $y_m^{(2)}$ the first three coefficients

$$c_1^{(2)} = c_0^{(2)}\Big[c^{-2} - \eta + \frac{\eta}{2}(\eta-1)\Big], \tag{12a}$$

$$c_2^{(2)} = -\frac{c_0^{(2)}}{2}\Big[(\eta-1)c^{-2} - \eta + \eta(\eta-1) - \frac{\eta}{6}(\eta-1)(\eta-2)\Big] \tag{12b}$$
$$+ \frac{c_1^{(2)}}{2}\Big[c^{-2} + 3 - 2\eta - \frac{\eta}{2}(\eta-1)\Big],$$

$$\begin{aligned} c_3^{(2)} = \frac{c_0^{(2)}}{3}\Big[&\Big(1+\frac{\eta}{2}(\eta-1)\Big)c^{-2} - \eta + \frac{3}{2}\eta(\eta-1) - \frac{\eta}{2}(\eta-1)(\eta-2) \\ &+ \frac{\eta}{24}(\eta-1)(\eta-2)(\eta-3)\Big] \\ - \frac{c_1^{(2)}}{3}&\Big[(\eta-1)c^{-2} - 7 - 6\eta + 2\eta(\eta-1) - \frac{\eta}{6}(\eta-1)(\eta-2)\Big] \\ + \frac{c_2^{(2)}}{3}&\Big[c^{-2} + 9 - 3\eta + \frac{\eta}{2}(\eta-1)\Big], \end{aligned} \tag{12c}$$

with $\eta = 1 + (2+d)/c$. Here $c_0^{(1)}$, $c_0^{(2)}$ denote arbitrary constants.

**Remark 1** *We remark that in the special case $c = 1$, $d = 0$ we obtain*

$$y_m^{(1)} = c_0^{(1)} \frac{m^{-4}}{(m-2)!}\Big(1 - \frac{3}{m} + \frac{21}{2m^2} - \frac{104}{3m^3} + \mathrm{O}\big(m^{-4}\big)\Big), \tag{13a}$$

$$y_m^{(2)} = c_0^{(2)}(m-2)!\, m^3 \Big(1 + \frac{1}{m} - \frac{3}{2m^2} - \frac{1}{3m^3} + \mathrm{O}\big(m^{-4}\big)\Big). \tag{13b}$$

**The explicit solution**. In most cases, second-order linear difference equations with variable coefficients cannot be solved in closed form. In this section we show that in the special case of the discrete Airy equation (6), it is possible to obtain an explicit solution. We present the derivation of this exact solution and study its asymptotic behaviour.

If one wants to solve a difference equation with polynomial coefficients (like (6)), one approach is to find the solution by the *"method of generating functions"* (cf. [9]); i.e., a generating function for a solution of (6) can be shown to satisfy a differential equation, which may be solvable in terms of known functions. To start with, define the generating function to be

$$g(\xi) = \sum_{m=-\infty}^{\infty} y_m \xi^m. \tag{14}$$

We multiply (6) with $\xi^{m-1}$ and sum it up for $m \in \mathbb{Z}$:

$$\sum_{m=-\infty}^{\infty} y_m \xi^{m-2} - (2+d)\sum_{m=-\infty}^{\infty} y_m \xi^{m-1} + \sum_{m=-\infty}^{\infty} y_m \xi^m - c \sum_{m=-\infty}^{\infty} m y_m \xi^{m-1} = 0.$$

This results in the following ordinary differential equation for $g$:

$$g'(\xi) - \frac{1-(2+d)\xi+\xi^2}{c\xi^2}\, g(\xi) = 0,$$

for which the solution is

$$g(\xi) = \xi^{-\frac{2+d}{c}}\, e^{(\xi-\frac{1}{\xi})/c} = \xi^{-\frac{2+d}{c}} \sum_{\nu=-\infty}^{\infty} J_\nu(\tfrac{2}{c})\xi^\nu.$$

Hence, the exact decaying solution of (6) is the *Bessel function* $J_\nu(\frac{2}{c})$ (regarded as function of its order $\nu$), i.e. the discrete Airy equation is nothing else but the recurrence relation for $J_\nu(\frac{2}{c})$. We note that it is well-known ([10], [20]) that the recurrence equation for the Bessel functions

$$J_{\nu+1}(z) - 2\,\frac{\nu}{z}\, J_\nu(z) + J_{\nu-1}(z) = 0, \tag{15}$$

still holds for complex orders $\nu$ and complex arguments $z$.

Thus the decaying solution to (6) can be represented as (cf. [20, Chapter 3.1]):

$$y_m = J_{m+\frac{2+d}{c}}(\tfrac{2}{c}) = \frac{1}{c^{m+\frac{2+d}{c}}} \sum_{n=0}^{\infty} \frac{(-1)^n}{c^{2n}\, n!\,\Gamma(m+\frac{2+d}{c}+n+1)}, \quad c,d \in \mathbb{C}. \tag{16}$$

We also observe that (14) is not a generating function in the strict sense but a *Laurent series*, which is uniformly convergent, i.e. differentiating each term is permissible (cf. [20]). Note that this generating function approach is not suitable for determining the growing solution of (6) for $m \to \infty$. This solution is the so-called *"Neumann-Function"* (or Bessel function of the second kind) which is known to also satisfy the recursion equation of the Bessel functions.

**Remark 2** *A difference equation more general than* (6) *was examined by Barnes [4] in 1904. He also considered* (6) *and found (through a different construction) the solution* (16).

The next step is to use (16) to examine the asymptotic behaviour of the discrete solutions. One can derive the following dominating series for the decaying solution:

$$|y_m| \le Y_m = \frac{1}{|c|^{m+\left|\frac{2+d}{c}\right|}} \frac{1}{\left|\Gamma(m+\frac{2+d}{c}+1)\right|}\, e^{\frac{1}{\left|c^2(m+\frac{2+d}{c}+1)\right|}}, \tag{17}$$

which can be estimated using Stirling's inequality

$$Y_m < \frac{1}{\sqrt{2\pi}} \frac{e^{\frac{1}{|c|^2}}}{|c|^{m+\frac{2+d}{c}}} \left(\frac{e}{m}\right)^m m^{-\frac{1}{2}} \frac{\Gamma(m+1)}{\Gamma(m+\frac{2+d}{c}+1)}, \tag{18}$$

if $(2+d)/c$ is a positive real number. We want to compare this result concerning the decay rate with the one derived by Mickens [15]. From setting $c = 1$, $d = 0$ in (18), it follows that

$$Y_m < \frac{e}{\sqrt{2\pi}} \frac{m^{-5/2}\, e^m}{m^m}, \tag{19}$$

and we see that the decay rate of (18) and (5) differs by a factor $m^{-6}$, i.e. our new bound $Y_m$ decays faster.

Another approach is to use an approximation for the exact solution of (6). We use the following asymptotic representation of Bessel functions for large values of the order $\nu$ (cf. [10]):

$$J_\nu(z) \approx \frac{1}{\sqrt{2\pi}}\, e^{\nu+\nu \log(z/2)-(\nu+1/2)\log\nu}, \quad |\nu| \to \infty, \quad |\arg\nu| \le \pi - \delta. \tag{20}$$

This enables us to give another asymptotic form of the recessive solution to the discrete model equation (6) with $c = 1$, $d = 0$:

$$y_m = J_{m+2}(2) \approx \frac{e^2}{\sqrt{2\pi}}\, e^m\, (m+2)^{-(m+5/2)}, \quad m \to \infty, \tag{21}$$

and with Stirling's formula this simplifies to $y_m \approx 1/(m+2)!$, $m \to \infty$.

## 3 Application to Parabolic Equation Calculations

With the results from the previous Section we want to derive a discrete transparent boundary condition (DTBC) for the so–called *standard "parabolic equation"* (SPE) [18], i.e. a one–way wave equation, arising for example in (underwater) acoustics and radiowave propagation problems. Here we concentrate on the application to underwater acoustics.

**The standard parabolic equation in underwater acoustics.** A standard task in oceanography is to calculate the acoustic pressure $p(z,r)$ emerging from a time–harmonic point source located in the water at $(z_s, 0)$. Here, $r > 0$ denotes the radial range variable and $0 < z < z_b$ the depth variable (assuming a cylindrical geometry). The water surface is at $z = 0$, and the (horizontal) sea bottom at $z = z_b$. We denote the local sound speed by $c(z,r)$, the density by $\rho(z,r)$, and the attenuation by $\alpha(z,r) \ge 0$. The *complex refractive index* is given by $N(z,r) = c_0/c(z,r) + i\alpha(z,r)/k_0$ with a reference sound speed $c_0$ and the reference wave number $k_0 = 2\pi f/c_0$, where $f$ denotes the frequency of the emitted sound.

The *SPE* in cylindrical coordinates $(z,r)$ reads:

$$2ik_0\psi_r(z,r) + \rho\,\partial_z(\rho^{-1}\partial_z)\psi(z,r) + k_0^2(N^2(z,r)-1)\,\psi(z,r) = 0, \tag{22}$$

where $\psi$ denotes the (complex valued) *outgoing acoustic field*

$$\psi(z,r) = \sqrt{k_0 r}\, p(z,r)\, e^{-ik_0 r}, \tag{23}$$

in the far field approximation ($k_0 r \gg 1$). This *Schrödinger equation* (22) is an evolution equation in $r$ and a reasonable description of waves with a propagation direction within about 15° of the horizontal.

Here, the physical problem is posed on the unbounded $z$–interval $(0,\infty)$ and one wishes to restrict the computational domain in the $z$–direction by introducing an artificial boundary at the water–bottom interface ($z = z_b$), where the wave propagation in water has to be coupled to the wave propagation in the the bottom. At the water surface one usually employs a Dirichlet ("pressure release") BC: $\psi(0,r) = 0$.

Since the density is typically discontinuous at the water–bottom interface ($z = z_b$), one requires continuity of the pressure and the normal particle velocity:

$$\psi(z_b-,r) = \psi(z_b+,r), \tag{24a}$$

$$\frac{\psi_z(z_b-,r)}{\rho_w} = \frac{\psi_z(z_b+,r)}{\rho_b}, \tag{24b}$$

where $\rho_w = \rho(z_b-,r)$ is the water density just above the bottom and $\rho_b$ denotes the constant density of the bottom.

In this work we are especially interested in the case of a *linear squared refractive index* in the bottom region. We denote the physical parameters in the bottom with the subscript $b$ and assume that the squared refractive index $N_b$ can be written as

$$N_b^2(z,r) = 1 + \beta + \mu(z - z_b), \quad z > z_b, \tag{25}$$

with real parameters $\beta$ and $\mu \neq 0$, i.e. no attenuation in the bottom: $\alpha_b = 0$. All other physical parameters are assumed to be constant in the bottom. Here, the slope $\mu > 0$ corresponds to a downward-refracting bottom (energy loss) and $\mu < 0$ represents the upward-refracting case, i.e. energy is returned from the bottom.

One can easily derive an estimate for the $L^2$–decay of solutions to the SPE, posed on the half-space $z > 0$. We assume $\rho = \rho(z)$ and a simple calculation (cf. [2]) gives

$$\partial_r \|\psi(.,r)\|^2 = -2c_0 \int_0^\infty \frac{\alpha}{c}\, |\psi|^2\, \rho^{-1}\, dz, \tag{26}$$

for the weighted $L^2$–norm ("acoustic energy")

$$\|\psi(.,r)\|^2 = \int_0^\infty |\psi(z,r)|^2\, \rho^{-1}(z)\, dz, \tag{27}$$

i.e. in the dissipation–free case ($\alpha \equiv 0$) $\|\psi(.,r)\|$ is conserved and for $\alpha > 0$ it decays.

## 4 Transparent Boundary Conditions

**Transparent Boundary Conditions.** In the following we will review from [13] the derivation of the transparent boundary condition at $z = z_b$ for the SPE with a linear squared refractive index. A transparent BC for the SPE (or Schrödinger equation) for a constant exterior medium was derived by several authors from various application fields, e.g. in [1].

If we further assume that the initial data $\psi^I = \psi(z,0)$, which models a point source located at $(z_s, 0)$, is supported in the *computational domain* $0 < z < z_b$, then a Laplace transformation in range of (22) for $z > z_b$ yields:

$$\hat{\psi}_{zz}(z,s) + [\mu k_0^2(z - \tilde{z}_b) + 2ik_0 s]\hat{\psi}(z,s) = 0, \quad z > z_b, \tag{28}$$

with $\tilde{z}_b = z_b - \beta/\mu$. Now the basic idea of the derivation is to explicitly solve the equation in the *exterior domain* $z > z_b$. Setting $\sigma^3 = -\mu k_0^2$ and $\tau = 2ik_0/\sigma^2$ (28) can be written as

$$\hat{\psi}_{zz}(z,s) + \sigma^2\Big[\sigma(z - \tilde{z}_b) + \tau s\Big]\hat{\psi}(z,s) = 0, \quad z > z_b. \tag{29}$$

Introducing the change of variables $\zeta_s(z) = \sigma(z - \tilde{z}_b) + \tau s$, $U(\zeta_s(z)) = \hat{\psi}(z,s)$, we can write (29) in the form of an *Airy equation*:

$$U''(\zeta_s(z)) + \zeta_s(z)\, U(\zeta_s(z)) = 0, \quad z > z_b. \tag{30}$$

The solution of (30) which decays for $z \to \infty$, for fixed $s$, Re $s > 0$ is

$$\hat{\psi}(z,s) = C_1(s)\ \mathrm{Ai}(\zeta_s(z)), \quad z > z_b, \tag{31}$$

if we define the physically relevant branch of $\sigma$ to be

$$\sigma = \begin{cases} (\mu k_0^2)^{1/3} e^{-i\pi/3}, & \mu > 0, \\ (-\mu k_0^2)^{1/3}, & \mu < 0. \end{cases} \tag{32}$$

Elimination of $C_1(s)$ gives

$$\hat{\psi}(z,s) = \hat{\psi}(z_{b}+, s)\, \frac{\mathrm{Ai}(\zeta_s(z))}{\mathrm{Ai}(\zeta_s(z_b))}, \quad z > z_b. \tag{33}$$

Finally, differentiation w.r.t. $z$ yields with the matching conditions (24) the *transformed transparent BC* at $z = z_b$:

$$\hat{\psi}_z(z_b-, s) = \frac{\rho_w}{\rho_b} s\, \hat{\psi}(z_b-, s)\, W(s), \qquad W(s) = \sigma\, \frac{\mathrm{Ai}'(\zeta_s(z_b))}{s\,\mathrm{Ai}(\zeta_s(z_b))}, \tag{34}$$

i.e. the *transparent BC* at $z = z_b$ reads:

$$\psi_z(z_b, r) = \frac{\rho_w}{\rho_b} \int_0^r \psi_r(z_b, r')\, g_\mu(r - r')\, dr'. \tag{35}$$

The kernel $g_\mu$ is obtained by an inverse Laplace transformation of $W(s)$ (cf. [6]):

$$g_\mu(r) = \sigma \left\{ \frac{\mathrm{Ai}'(\zeta_0(z_b))}{\mathrm{Ai}(\zeta_0(z_b))} + \sum_{j=1}^{\infty} \frac{e^{-(a_j - \zeta_0(z_b)) r/\tau}}{a_j - \zeta_0(z_b)} \right\}, \tag{36}$$

where $\zeta_0(z_b) = \sigma\beta/\mu$ and the $(a_j)$ are the zeros of the Airy function Ai which are all located on the negative real axis [17]. This BC is *nonlocal* in the range variable $r$ and can easily be discretized, e.g. in conjunction with a finite difference scheme for (22). The constant term in $g_\mu$ acts like a Dirac function and the infinite series represents the continuous part. As Levy noted in [14] the kernel $g_\mu$ decays extremely fast for $\mu > 0$ and for negative $\mu$ it decays slowly at short ranges and then oscillates.

**Numerical Implementation.** Now we shall discuss how to solve (22) numerically with a *Crank-Nicolson* finite difference scheme which is of second order (in $\Delta z$ and $\Delta r$) and unconditionally stable. We will use the uniform grid $z_j = jh$, $r_n = nk$ with $h = \Delta z$, $k = \Delta r$ and the approximations $\psi_j^{(n)} \approx \psi(z_j, r_n)$, $\rho_j \approx \rho(z_j)$. The discretized SPE (22) then reads:

$$-iR(\psi_j^{(n+1)} - \psi_j^{(n)}) = \rho_j \Delta_z^0 (\rho_j^{-1} \Delta_z^0)(\psi_j^{(n+1)} + \psi_j^{(n)}) + w\Big((N^2)_j^{(n)} - 1\Big)(\psi_j^{(n+1)} + \psi_j^{(n)}), \tag{37}$$

with $\Delta_z^0 \psi_j^{(n)} = \psi_{j+1/2}^{(n)} - \psi_{j-1/2}^{(n)}$, the mesh ratio $R = 4k_0 h^2/k$ and $w = k_0^2 h^2$.

**Discretization of the continuous TBC.** To incorporate the TBC (35) in a finite difference scheme we make the approximation that $\psi_r(z_b, r')$ is constant on each subinterval $r_n < r' < r_{n+1}$ and integrate the kernel $g_\mu$ exactly. In the following we review the discretization from [14] and start with the discretization in range:

$$\psi_z(z_b, r_n) = \frac{\rho_w}{\rho_b} \sum_{m=0}^{n-1} \frac{\psi_b^{(n-m)} - \psi_b^{(n-m-1)}}{k} G_m, \tag{38}$$

where we have set $\psi_b^{(n)} = \psi(z_b, r_n)$ and $G_m$ is given by

$$G_m = \int_{r_m}^{r_{m+1}} g_\mu(\eta)\, d\eta = k\sigma \frac{\mathrm{Ai}'(\zeta_0(z_b))}{\mathrm{Ai}(\zeta_0(z_b))} + \frac{2ik_0}{\sigma} \sum_{j=1}^{\infty} \frac{e^{-(a_j - \zeta_0(z_b)) r/\tau}}{(a_j - \zeta_0(z_b))^2} \Bigg|_{r=r_m}^{r=r_{m+1}}. \tag{39}$$

This leads after rearranging to

$$k\frac{\rho_b}{\rho_w}\psi_z(z_b,r_n) = -\psi_b^{(0)}G_n + \psi_b^{(n)}G_0 + \sum_{m=1}^{n-1}\psi_b^{(n-m)}(G_m - G_{m-1}) \tag{40}$$

In [14] Levy used an *offset grid* in depth, i.e. $\tilde{z}_j = (j+\frac{1}{2})h$, $\tilde{\psi}_j^{(n)} \approx \psi(\tilde{z}_j, r_n)$, $j=-1,\dots,J$, where the water–bottom interface lies between the grid points $j=J-1$ and $J$:

$$\psi_b^{(m)} = \psi(z_b,r_m) \approx \frac{\tilde{\psi}_J^{(m)} + \tilde{\psi}_{J-1}^{(m)}}{2}, \quad \psi_z(z_b,r_n) \approx \frac{\tilde{\psi}_J^{(n)} - \tilde{\psi}_{J-1}^{(n)}}{h}. \tag{41}$$

This yields finally (recall that $\tilde{\psi}_J^{(0)} = \tilde{\psi}_{J-1}^{(0)} = 0$) the following *discretized TBC* for the SPE:

$$(1-b_0)\tilde{\psi}_J^{(n)} - (1+b_0)\tilde{\psi}_{J-1}^{(n)} = \sum_{m=1}^{n-1} b_m(\tilde{\psi}_J^{(n-m)} + \tilde{\psi}_{J-1}^{(n-m)}), \tag{42}$$

with

$$b_0 = \frac{1}{2}\frac{h}{k}\frac{\rho_w}{\rho_b}G_0, \quad b_m = \frac{1}{2}\frac{h}{k}\frac{\rho_w}{\rho_b}(G_m - G_{m-1}). \tag{43}$$

Note that the constant term in (39) enters only $b_0$. Since $a_j \sim -\Bigl(\frac{3\pi}{8}(4j-1)\Bigr)^{2/3}$ for $j\to\infty$ the series (39) defining $G_m$ has good convergence properties for positive range $r$ but for $r=0$ the convergence is very slow. To overcome this numerical problem we use the identity

$$\sum_{j=1}^{\infty}\frac{1}{(a_j-\zeta_0(z_b))^2} = \left(\frac{\mathrm{Ai}'(\zeta_0(z_b))}{\mathrm{Ai}(\zeta_0(z_b))}\right)^2 - \zeta_0(z_b), \tag{44}$$

which can be derived analogously to the one in [13].

In a numerical implementation one has to limit the summation in (36) and therefore the TBC is not fully transparent any more. Moreover, the stability of the resulting scheme is not clear since the discretized TBC (42) is not matched to the finite difference scheme (37) in the interior domain. Instead of using an ad–hoc discretization of the analytic transparent BC like in [14] we will construct *discrete TBCs* of the fully discretized half–space problem with the help of the results from Section 2.

**Discrete transparent boundary conditions.** To derive the discrete TBC we will now mimic the derivation of the analytic TBC from Section 2 on a discrete level. In analogy to the continuous problem we assume for the initial data $\psi_j^0 = 0$, $j \geq J-1$ and use the linear potential term $(N^2)_j^{(n)} - 1 = \beta + \mu h(j-J)$, $z_b = Jh$ and solve the *discrete exterior problem*

$$-iR(\psi_j^{(n+1)} - \psi_j^{(n)}) = \Delta^2\psi_j^{(n+1)} + \Delta^2\psi_j^{(n)} + w\Bigl[\beta+\mu h(j-J)\Bigr](\psi_j^{(n+1)} + \psi_j^{(n)}), \tag{45}$$

$j \geq J-1$, $\Delta^2 \psi_j^{(n)} = \psi_{j+1}^{(n)} - 2\,\psi_j^{(n)} + \psi_{j-1}^{(n)}$, by using the $Z$–transformation:

$$\mathcal{Z}\{\psi_j^{(n)}\} = \hat{\psi}_j(z) := \sum_{n=0}^{\infty} \psi_j^{(n)}\, z^{-n}, \quad z \in \mathbb{C}, \quad |z| > 1. \tag{46}$$

Hence, the $Z$–transformed finite difference scheme (37), for $j \geq J$, is a *discrete Airy equation*

$$\hat{\psi}_{j+1}(z) - 2\Big[1 - i\zeta(z) - \mu \frac{k_0^2}{2} h^3 (j-J)\Big]\hat{\psi}_j(z) + \hat{\psi}_{j-1}(z) = 0, \quad j \geq J-1, \tag{47}$$

with

$$\zeta(z) = \frac{R}{2}\frac{z-1}{z+1} - i\frac{\beta}{2}k_0^2 h^2. \tag{48}$$

Comparing (47) with the recurrence relation of the Bessel function $J_\nu(\sigma)$ yields the condition

$$\frac{\nu}{\sigma} = 1 - i\zeta(z) - \mu\frac{k_0^2}{2}h^3(j-J) \stackrel{!}{=} \frac{j + \text{offset}}{\sigma}, \tag{49}$$

and we conclude that the exact solution of (47) is

$$\hat{\psi}_j(z) = J_{\nu_j(z)}(\sigma), \tag{50}$$

with

$$\nu = \nu_j(z) = \sigma(1 - i\zeta(z)) + j - J, \quad \sigma = -\Big(\mu\frac{k_0^2}{2}h^3\Big)^{-1} \in \mathbb{R}. \tag{51}$$

From (50) we obtain the *transformed discrete TBC* at $z_b = Jh$:

$$\hat{\psi}_{J-1}(z) = \hat{g}_{\mu,J}(z)\hat{\psi}_J(z) \quad \text{with} \quad \hat{g}_{\mu,J}(z) = \frac{J_{\nu_{J-1}(z)}(\sigma)}{J_{\nu_J(z)}(\sigma)} = \frac{J_{\sigma(1-i\zeta(z))-1}(\sigma)}{J_{\sigma(1-i\zeta(z))}(\sigma)}. \tag{52}$$

Finally, an inverse $Z$–transformation yields the *discrete TBC*

$$\psi_{J-1}^{(n)} - \ell_J^{(0)}\psi_J^{(n)} = \sum_{m=1}^{n-1} \psi_J^{(n-m)}\,\ell_J^{(m)}, \tag{53}$$

with

$$\ell_J^{(n)} = \mathcal{Z}^{-1}\left\{\hat{g}_{\mu,J}(z)\right\} = \frac{\tau^n}{2\pi}\int_0^{2\pi} \hat{g}_{\mu,J}(\tau e^{i\varphi})e^{in\varphi}\,d\varphi, \quad n \in \mathbb{Z}_0, \quad \tau > 0. \tag{54}$$

Since this inverse $Z$-transformation cannot be done explicitly, we use a numerical inversion technique based on FFT (cf. [8]); for details of this routine we refer the reader to [7]. Note that the Bessel functions in (52) with complex order and (possibly large) real argument can be evaluated by special software packages (see e.g. [19]).

Since the magnitude of $\ell_J^{(n)}$ does not decay as $n \to \infty$ (Im $\ell_J^{(n)}$ behaves like const $\cdot(-1)^n$ for large $n$), it is more convenient to use a modified formulation of the DTBCs (cf. [8]). We introduce the *summed coefficients*

$$s_J^{(n)} = \mathcal{Z}^{-1}\left\{\hat{s}_J(z)\right\}, \text{ with } \hat{s}_J(z) := \frac{z+1}{z}\hat{\ell}_J(z), \tag{55}$$

which satisfy

$$s_J^{(0)} = \ell_J^{(0)}, \quad s_J^{(n)} = \ell_J^{(n)} + \ell_J^{(n-1)}, \quad n \geq 1. \tag{56}$$

In physical space, the DTBC is:

$$\psi_{J-1}^{(n)} - s_J^{(0)}\psi_J^{(n)} = \sum_{m=1}^{n-1} s_J^{(n-m)}\psi_J^{(m)} - \psi_{J-1}^{(n-1)}, \quad n \geq 1. \tag{57}$$

In the following, we will present two alternative approaches to obtain a DTBC: asymptotic expansions and a continued fraction formula.

**Asymptotic Expansions.** For a *second approach* to obtain an approximated DTBC, one can use *asymptotic expansions*. Using the asymptotic formula (20) leads to the approximate DTBC

$$\hat{\psi}_{J-1}(z) = \hat{h}_{\mu,J}(z)\hat{\psi}_J(z) \quad \text{with} \quad \hat{h}_{\mu,J}(z) = \frac{2}{e}\sigma^{-1}\sqrt{\nu_J(\nu_J-1)}\Big(\frac{\nu_J}{\nu_J-1}\Big)^{\nu_J}, \tag{58}$$

with $\nu_J$, $\sigma$ given by (51).

Alternatively, one can use the asymptotic solution $y_m^{(1)}$ from (9a). The $Z$–transformed scheme in the exterior $j \geq J-1$, given by (47), is a discrete Airy equation of the form (6) with

$$c = 2\sigma^{-1}, \quad d = -2i\zeta(z) - cJ, \text{ i.e. } \theta = 2 + \frac{2+d}{c} = 2 + \nu_0,$$

and thus we obtain an approximation to the transformed DTBC of the form

$$\hat{\psi}_{J-1}(z) = \hat{k}_{\mu,J}(z)\hat{\psi}_J(z), \tag{59a}$$

with

$$\hat{k}_{\mu,J}(z) = \frac{y_{J-1}^{(1)}}{y_J^{(1)}} = c(J-2)\Big(\frac{J}{J-1}\Big)^{\theta}\frac{\sum_{s=1}^{\infty}\frac{c_s^{(1)}}{(J-1)^s}}{\sum_{s=1}^{\infty}\frac{c_s^{(1)}}{J^s}}. \tag{59b}$$

**Continued fraction formula.** Finally, for a *third approach* for an approximation to the DTBC, we use a *continued fraction formulation*. We can easily deduce an expression for the quotient of Bessel functions (like (52)) as a continued fraction from the recurrence formula (15). If we rewrite (15) as

$$\frac{J_{\nu-1}(z)}{J_\nu(z)} = 2\nu z^{-1} - \frac{1}{\frac{J_\nu(z)}{J_{\nu+1}(z)}},$$

it is obvious that

$$\frac{J_{\nu-1}(z)}{J_\nu(z)} = 2\nu z^{-1} - \frac{1}{2(\nu+1)z^{-1}-} \cdots \frac{1}{2(\nu+M)z^{-1}-} \frac{J_{\nu+M-1}(z)}{J_{\nu+M}(z)}.$$

This holds for general values of $\nu$ and it can be shown, with the help of the theory of Lommel polynomials [20, Section 9.65], that when $M \to \infty$, the last quotient may be neglected, so that

$$\frac{J_{\nu-1}(z)}{J_\nu(z)} = 2\nu z^{-1} - \frac{1}{2(\nu+1)z^{-1}-} \frac{1}{2(\nu+2)z^{-1}-\cdots}. \tag{60}$$

This continued fractions formula offers another way to evaluate the quotient of two Bessel functions needed in the transformed discrete TBC (52). For the numerical implementation we use the *modified Lentz's method* [12] which is an efficient general method for evaluating continued fractions.

**Remark 3** *For brevity of the presentation, we omit here the discussion of an adequate discrete treatment of the typical density shock at $z = z_b$ and refer the reader to [2] for a detailed discussion of various strategies.*

## 5 Approximation by Sums of Exponentials

An ad-hoc implementation of the discrete convolution (57) with convolution coefficients $s_J^{(n)}$ from (55) (or obtained by any of the above approaches) has still one disadvantage. The boundary condition is non–local and therefore computational expensive. As a remedy, we proposed in [3] the sum-of-exponentials ansatz. In the sequel we will briefly review this ansatz.

In order to derive a fast numerical method to calculate the discrete convolutions in (57), we approximate the coefficients $s_J^{(n)}$ by the following ansatz (*sum of exponentials*):

$$s_J^{(n)} \approx \tilde{s}_J^{(n)} := \begin{cases} s_J^{(n)}, & n = 0,1 \\ \sum_{l=1}^{L} b_l \, q_l^{-n}, & n = 2,3,\dots, \end{cases} \tag{61}$$

where $L \in \mathbb{N}$ is a fixed number. Evidently, the approximation properties of

$\tilde{s}_J^{(n)}$ depend on $L$, and the corresponding set $\{b_l, q_l\}$. Below we propose a deterministic method of finding $\{b_l, q_l\}$ for fixed $L$.

Let us fix $L$ and consider the formal power series:

$$g(x) := s_J^{(2)} + s_J^{(3)} x + s_J^{(4)} x^2 + \dots, \quad |x| \le 1. \tag{62}$$

If there exists the $[L-1|L]$ *Padé approximation*

$$\tilde{g}(x) := \frac{P_{L-1}(x)}{Q_L(x)} \tag{63}$$

of (62), then its Taylor series

$$\tilde{g}(x) = \tilde{s}_J^{(2)} + \tilde{s}_J^{(3)} x + \tilde{s}_J^{(4)} x^2 + \dots \tag{64}$$

satisfies the conditions

$$\tilde{s}_J^{(n)} = s_J^{(n)}, \qquad n = 2, 3, \dots, 2L+1, \tag{65}$$

due to the definition of the Padé approximation rule.

**Theorem 4 ([3])** *Let $Q_L(x)$ have $L$ simple roots $q_l$ with $|q_l| > 1$, $l = 1, \dots, L$. Then*

$$\tilde{s}_J^{(n)} = \sum_{l=1}^{L} b_l \, q_l^{-n}, \qquad n = 2, 3, \dots, \tag{66}$$

*where*

$$b_l := -\frac{P_{L-1}(q_l)}{Q'_L(q_l)} \, q_l \ne 0, \qquad l = 1, \dots, L. \tag{67}$$

It follows from (65) and (66) that the set $\{b_l, q_l\}$ defined in Theorem 4 can be used in (61) at least for $n = 2, 3, .., 2L+1$. The main question now is: Is it possible to use these $\{b_l, q_l\}$ also for $n > 2L+1$? In other words, what quality of approximation

$$\tilde{s}_J^{(n)} \approx s_J^{(n)}, \qquad n > 2L+1 \tag{68}$$

can we expect?

The above analysis permits us to give the following description of the approximation to the convolution coefficients $s_J^{(n)}$ by the representation (61) if we use a $[L-1|L]$ Padé approximant to (62): the first $2L$ coefficients are reproduced exactly, see (65); however, the asymptotic behaviour of $s_J^{(n)}$ and $\tilde{s}_J^{(n)}$ (as $n \to \infty$) differs strongly (algebraic versus exponential decay). A typical graph of $|s_J^{(n)} - \tilde{s}_J^{(n)}|$ versus $n$ for $L = 27$ is shown in Fig. 2 in Section 7.

**Fast Evaluation of the Discrete Convolution.** Let us consider the approximation (61) of the discrete convolution kernel appearing in the DTBC

(57). With these “exponential” coefficients the convolution

$$C^{(n)} := \sum_{m=1}^{n-1} \tilde{s}_J^{(n-m)} \psi_J^{(m)}, \quad \tilde{s}_J^{(n)} = \sum_{l=1}^{L} b_l \, q_l^{-n}, \tag{69}$$

$|q_l| > 1$, of a discrete function $\psi_J^{(m)}$, $m = 1, 2, \dots$, with the kernel coefficients $\tilde{s}_J^{(n)}$, can be calculated by recurrence formulas, and this will reduce the numerical effort significantly (cf. Fig. 6 in Section 7).

A straightforward calculation (cf. [3]) yields: The value $C^{(n)}$ from (69) for $n \geq 2$ is represented by

$$C^{(n)} = \sum_{l=1}^{L} C_l^{(n)}, \tag{70}$$

where

$$\begin{aligned} C_l^{(1)} &\equiv 0, \\ C_l^{(n)} &= q_l^{-1} C_l^{(n-1)} + b_l \, q_l^{-1} \psi_J^{(n-1)}, \end{aligned} \tag{71}$$

$n = 2, 3, \dots \; l = 1, \dots, L.$

Finally we summarize the approach by the following algorithm:

1. calculate $s_J^{(n)}, n = 0, \dots, N-1$, via numerical inverse $Z$-transformation;
2. calculate $\tilde{s}_J^{(n)}$ via Padé–algorithm;
3. the corresponding coefficients $b_l$, $q_l$ are used for the efficient calculation of the discrete convolutions.

## 6 Stability Analysis of the numerical scheme

Here we analyze the stability of our numerical scheme for the SPE (37) along with a surface condition and the the DTBC (53):

$$\begin{cases} -iR(\psi_j^{(n+1)} - \psi_j^{(n)}) = \rho_j \Delta_z^0 (\rho_j^{-1} \Delta_z^0)(\psi_j^{(n+1)} + \psi_j^{(n)}) + w\Big[(N^2)_j^{(n)} - 1\Big](\psi_j^{(n+1)} + \psi_j^{(n)}) \\ \qquad\qquad\qquad\qquad\qquad\qquad j = 1, \dots, J-1, \\ \psi_j^{(0)} = \psi^I(z_j), \; j = 0, 1, 2, \dots, J-1, J; \\ \text{with } \psi_{J-1}^{(0)} = \psi_J^{(0)} = 0, \\ \psi_0^{(n)} = 0, \\ \hat{\psi}_{J-1}(z) = \hat{g}_{\mu,J}(z) \hat{\psi}_J(z), \end{cases} \tag{72}$$

where $\hat{g}_{\mu,J}(z)$ is given by (52).

In the sequel we want to derive an a-priori estimate of the discrete solution in the discrete weighted $\ell^2$–norm:

$$\|\psi^{(n)}\|_2^2 := h \sum_{j=1}^{J-1} |\psi_j^{(n)}|^2 \rho_j^{-1}, \tag{73}$$

which is the discrete analogue to (27). The following theorem bounds the exponential growth of solutions to the numerical scheme for a fixed discretization.

**Theorem 5** ***(Growth condition)*** *Let the boundary kernel $\hat{g}_{\mu,J}$ satisfy*

$$\operatorname{Im} \hat{g}_{\mu,J}(\gamma e^{i\varphi}) \leq 0, \quad \forall\, 0 \leq \varphi \leq 2\pi, \tag{74}$$

*for some (sufficiently large) $\gamma \geq 1$ (i.e. the system is dissipative). Assume also that $\hat{g}_{\mu,J}(z)$ is analytic for $|z| \geq \gamma$. Then, the solution of (72) satisfies the a-priori estimate*

$$\|\psi^{(n)}\|_2 \leq \|\psi^0\|_2\, \gamma^n, \quad n \in \mathbb{N}. \tag{75}$$

**PROOF.** The proof is based on a discrete energy estimate for the new variable

$$\phi_j^{(n)} := \psi_j^{(n)}\, \gamma^{-n},$$

which satisfies the equation

$$\begin{aligned}
-iR(\phi_j^{(n+1)} - \phi_j^{(n)}) &= \Big(\rho_j \Delta_z^0(\rho_j^{-1}\Delta_z^0) + w\big[(N^2)_j^{(n)} - 1\big]\Big)\,(\phi_j^{(n+1)} + \phi_j^{(n)}) \qquad \text{(76a)}\\
&\quad + (\gamma - 1)\Big(\rho_j \Delta_z^0(\rho_j^{-1}\Delta_z^0) + w\big[(N^2)_j^{(n)} - 1\big] + iR\Big)\,\phi_j^{(n+1)},\\
&\quad j = 1, \dots, J-1,\\
\phi_j^{(0)} &= \psi_j^{(0)}, \quad j = 0, \dots, J, \qquad \text{(76b)}\\
\phi_0^{(n)} &= 0, \qquad \text{(76c)}\\
\Delta^- \hat{\phi}_J(z) &= -(\hat{g}_{\mu,J}(\gamma z) - 1)\, \hat{\phi}_J(z). \qquad \text{(76d)}
\end{aligned}$$

In physical space, the bottom BC can be written as

$$\Delta^- \phi_J^{(n)} = -\phi_J^{(n)} * \frac{\tilde{\ell}_J^{(n)}}{\gamma^n} = -\sum_{m=0}^{n} \phi_J^{(m)} \left(\tilde{\ell}_J^{(n-m)}\, \gamma^{m-n}\right). \tag{77}$$

First we multiply (76a) by $\bar{\phi}_j^{(n)} \rho_j^{-1}/\gamma$ and its complex conjugate by $\phi_j^{(n+1)} \rho_j^{-1}$:

$$\begin{aligned}
iR\Big(|\phi_j^{(n)}|^2 - \bar{\phi}_j^{(n)}\phi_j^{(n+1)}\Big)\rho_j^{-1} &=\\
&\bar{\phi}_j^{(n)}\Big(\Delta_z^0(\rho_j^{-1}\Delta_z^0) + w\big[(N^2)_j^{(n)} - 1\big]\rho_j^{-1}\Big)\,\Big(\phi_j^{(n+1)} + \phi_j^{(n)}\Big)\\
&+(\gamma^{-1} - 1)\bar{\phi}_j^{(n)}\,\Big(\Delta_z^0(\rho_j^{-1}\Delta_z^0) + \Big(w\big[(N^2)_j^{(n)} - 1\big] - iR\Big)\rho_j^{-1}\Big)\,\phi_j^{(n)},
\end{aligned} \tag{78a}$$

$$
\begin{aligned}
iR\Big(|\phi_j^{(n+1)}|^2 - \bar\phi_j^{(n)}\phi_j^{(n+1)}\Big)\rho_j^{-1} = {}&\\
&\phi_j^{(n+1)}\Big(\Delta_z^0(\rho_j^{-1}\Delta_z^0) + w\big[\overline{(N^2)_j^{(n)}}-1\big]\rho_j^{-1}\Big)\left(\bar\phi_j^{(n+1)} + \bar\phi_j^{(n)}\right)\\
&\quad+(\gamma-1)\phi_j^{(n+1)}\Big(\Delta_z^0(\rho_j^{-1}\Delta_z^0) + \Big(w\big[\overline{(N^2)_j^{(n)}}-1\big] - iR\Big)\rho_j^{-1}\Big)\,\bar\phi_j^{(n+1)}.
\end{aligned}
\tag{78b}
$$

Next we subtract (78a) from (78b), sum from $j=1$ to $j=J-1$, and apply summation by parts:

$$
\begin{aligned}
iR\sum_{j=1}^{J-1}\Big(|\phi_j^{(n+1)}|^2 - |\phi_j^{(n)}|^2\Big)\rho_j^{-1} = {}& -\sum_{j=1}^{J-1}\Big(|\Delta^-\phi_j^{(n+1)}|^2 - |\Delta^-\phi_j^{(n)}|^2\Big)\rho_{j-1/2}^{-1}\\
&+\Big[\phi_{J-1}^{(n+1)}\Delta^-\Big(\bar\phi_J^{(n+1)} + \bar\phi_J^{(n)}\Big) - \bar\phi_{J-1}^{(n)}\Delta^-\Big(\phi_J^{(n+1)} + \phi_J^{(n)}\Big)\Big]\rho_{J-1/2}^{-1}\\
&+w\sum_{j=1}^{J-1}\Big(\big[\overline{(N^2)_j^{(n)}}-1\big](|\phi_j^{(n+1)}|^2 + \bar\phi_j^{(n)}\phi_j^{(n+1)}) - \big[(N^2)_j^{(n)}-1\big](|\phi_j^{(n)}|^2 + \bar\phi_j^{(n)}\phi_j^{(n+1)})\Big)\rho_j^{-1}\\
&+w\sum_{j=1}^{J-1}\Big((\gamma-1)\big[\overline{(N^2)_j^{(n)}}-1\big]|\phi_j^{(n+1)}|^2 + (1-\gamma^{-1})\big[(N^2)_j^{(n)}-1\big]|\phi_j^{(n)}|^2\Big)\rho_j^{-1}\\
&-iR\sum_{j=1}^{J-1}\Big((\gamma-1)|\phi_j^{(n+1)}|^2 + (1-\gamma^{-1})|\phi_j^{(n)}|^2\Big)\rho_j^{-1}\\
&-(\gamma-1)\sum_{j=1}^{J-1}|\Delta^-\phi_j^{(n+1)}|^2\rho_j^{-1} - (1-\gamma^{-1})\sum_{j=1}^{J-1}|\Delta^-\phi_j^{(n)}|^2\rho_j^{-1}\\
&+\Big[(\gamma-1)\phi_{J-1}^{(n+1)}\Delta^-\bar\phi_J^{(n+1)} + (1-\gamma^{-1})\bar\phi_{J-1}^{(n)}\Delta^-\phi_J^{(n)}\Big]\rho_{J-1/2}^{-1}
\end{aligned}
\tag{79}
$$

Now, taking imaginary parts one obtains after a lengthy calculation:

$$
\begin{aligned}
\sum_{j=1}^{J-1}\left(|\phi_j^{(n+1)}|^2 - |\phi_j^{(n)}|^2\right)\rho_j^{-1} = {}& -(\gamma-1)\sum_{j=1}^{J-1}|\phi_j^{(n+1)}|^2\rho_j^{-1} - (1-\gamma^{-1})\sum_{j=1}^{J-1}|\phi_j^{(n)}|^2\rho_j^{-1}\\
&-\frac{w}{\gamma R}\sum_{j=1}^{J-1}\mathrm{Im}\left[(N^2)_j^{(n)}-1\right]|\phi_j^{(n)} + \gamma\phi_j^{(n+1)}|^2\rho_j^{-1}\\
&-\frac{1}{\gamma R\rho_{J-1/2}}\,\mathrm{Im}\left[\Big(\bar\phi_J^{(n)} + \gamma\bar\phi_J^{(n+1)}\Big)\Delta^-\Big(\phi_J^{(n)} + \gamma\phi_J^{(n+1)}\Big)\right].
\end{aligned}
\tag{80}
$$

Summing (80) from $n = 0$ to $n = N$ yields (note that $\gamma \geq 1$):

$$\begin{aligned}
\|\phi^{(N+1)}\|_2^2 \leq \|\phi^{(0)}\|_2^2 &- \frac{wh}{\gamma^2 R} \sum_{n=0}^{N} \sum_{j=1}^{J-1} \operatorname{Im}\left[(N^2)_j^{(n)} - 1\right] |\phi_j^{(n)} + \gamma \phi_j^{(n+1)}|^2 \rho_j^{-1} \\
&- \frac{h}{\gamma^2 R \rho_{J-1/2}} \operatorname{Im} \sum_{n=0}^{N} (\bar{\phi}_J^{(n)} + \gamma \bar{\phi}_J^{(n+1)}) \Delta^- (\phi_J^{(n)} + \gamma \phi_J^{(n+1)}) \\
= \|\phi^{(0)}\|_2^2 &- \frac{kh}{2\gamma^2} \sum_{n=0}^{N} \sum_{j=1}^{J-1} \alpha_j^{(n+1/2)} \frac{c_0}{c_j^{(n+1/2)}} |\phi_j^{(n)} + \gamma \phi_j^{(n+1)}|^2 \rho_j^{-1} \\
&+ \frac{k}{4\gamma^2 k_0 h \rho_{J-1/2}} \operatorname{Im} \sum_{n=0}^{N} (\bar{\phi}_J^{(n)} + \gamma \bar{\phi}_J^{(n+1)}) \, (\phi_J^{(n)} + \gamma \phi_J^{(n+1)}) * \frac{\tilde{\ell}_J^{(n)}}{\gamma^n}.
\end{aligned} \tag{81}$$

For the last identity we used the bottom BC (77) and $\phi_0^{(0)} = \phi_J^{(0)} = 0$.

Since $\alpha_j^{(n+1/2)} \geq 0$, it remains to determine the sign of the last term in (81) to finish the proof. To this end we define (for $N$ fixed) the two sequences,

$$u^{(n)} := \begin{cases} \phi_J^{(n)} + \gamma \phi_J^{(n+1)}, & n = 0, \dots, N, \\ 0, & n > N, \end{cases}$$

$$v^{(n)} := u^{(n)} * \frac{\tilde{\ell}_J^{(n)}}{\gamma^n} = \sum_{m=0}^{n} u^{(m)} \frac{\tilde{\ell}_J^{(n-m)}}{\gamma^{n-m}}, \quad n \in \mathbb{N}_0.$$

The $Z$–transform $\mathcal{Z}\{u^{(n)}\} = \hat{u}(z)$ is analytic for $|z| > 0$, since it is a finite sum. The $Z$–transform $\mathcal{Z}\{v^{(n)}\}$ then satisfies $\hat{v}(z) = (\hat{g}_{\mu,J}(\gamma z) - 1)\hat{u}(z)$ and is analytic for $|z| \geq 1$. Using Plancherel's Theorem for $Z$–transforms we have

$$\begin{aligned}
\sum_{n=0}^{N} v^{(n)} \bar{u}^{(n)} = \sum_{n=0}^{\infty} v^{(n)} \bar{u}^{(n)} &= \frac{1}{2\pi} \int_0^{2\pi} \hat{v}(e^{i\varphi}) \overline{\hat{u}(e^{i\varphi})} \, d\varphi \\
&= \frac{1}{2\pi} \int_0^{2\pi} |\hat{u}(e^{i\varphi})|^2 \Big(\hat{g}_{\mu,J}(\gamma e^{i\varphi}) - 1\Big) \, d\varphi.
\end{aligned} \tag{82}$$

Using (82) for the boundary term in (81) now gives:

$$\begin{aligned}
\|\phi^{(N+1)}\|_2^2 &\leq \|\phi^{(0)}\|_2^2 \\
&+ \frac{h}{2\pi R \gamma^2 \rho_{J-1/2}} \int_0^{2\pi} |(1 + \gamma e^{i\varphi}) \hat{\phi}_J(e^{i\varphi})|^2 \operatorname{Im}\Big(\hat{g}_{\mu,J}(\gamma e^{i\varphi}) - 1\Big) \, d\varphi.
\end{aligned} \tag{83}$$

Our assumption on $\hat{g}_{\mu,J}$ therefore implies

$$\|\phi^{(N)}\|_2 \leq \|\phi^{(0)}\|_2, \quad \forall \, N \geq 0,$$

and the result of the theorem follows.

**Remark 6** *Above we have assumed that the $Z$-transformed boundary kernel $\hat{g}_{\mu,J}(z)$ is analytic for $|z| \geq \beta$. Hence its imaginary parts is a harmonic functions there. Since the average of $\hat{g}_{\mu,J}(z)$ on the circles $z = \beta e^{i\varphi}$ equals $g^{(0)}_{\mu,J} = \hat{g}_{\mu,J}(z = \infty)$, condition (74) implies Im $\hat{g}_{\mu,J}(z = \infty) \leq 0$. Then we have the following simple consequence of the maximum principle for the Laplace equation:*

*If condition (74) holds for some $\beta_0$, it also holds for all $\beta > \beta_0$.*

## 7 Numerical Example

In the example of this Section we will consider the SPE for comparing the numerical result from using our new (approximated) discrete TBC to the solution using the discretized TBC of Levy [13]. We used the environmental test data from [6] and the Gaussian beam from [11] as starting field $\psi^I$. Below we present the so-called *transmission loss* $-10\log_{10}|p|^2$, where the acoustic pressure $p$ is calculated from (23). We computed a *reference solution* on a three times larger computational domain confined with the DTBC from [2].

**Example.** As an illustrating example we chose the typical *downward refracting case* (i.e. energy loss to the bottom): $\mu = 2 \cdot 10^{-4}\,\mathrm{m}^{-1}$. The source at the depth $z_s = 91.44\,\mathrm{m}$ is emitting sound with a frequency $f = 300\,\mathrm{Hz}$ and the receiver is located at the depth $z_r = 27.5\,\mathrm{m}$. The TBC is applied at $z_b = 152.5\,\mathrm{m}$ and the discretization parameters are given by $\Delta r = 10\,\mathrm{m}$, $\Delta z = 0.5\,\mathrm{m}$. It contains no attenuation: $\alpha = 0$. We consider a range-independent situation for $0 < r < 50\,\mathrm{km}$, i.e. 5000 range steps. The sound speed varies linearly from $c(0\,\mathrm{m}) = 1536.5\,\mathrm{m\,s^{-1}}$ to $c(152.5\,\mathrm{m}) = 1539.24\,\mathrm{m\,s^{-1}}$. The reference sound speed $c_0$ is chosen to be equal to $c(z_b)$ such that $\beta = 0$ in (25).

For this choice of parameters the mesh ratio becomes $R \approx 0.12246$ and the parameter $\sigma \approx -53345.32$; that is, the value of $\nu_J$ defined in (51) is much too large for the routines like COULCC [19] for evaluating Bessel functions. On the other hand, using the asymptotic formula (58) is not advisable since for large $\nu_J$ we have $\hat{h}_{\mu,J}(z) \sim 2(1 - i\zeta(z))$ which is only the first term in the continued fraction expansion (60). Therefore, we decided to evaluate the ratio of the two Bessel functions in (52) by the continued fraction formula (60) together with the sum-of-exponentials ansatz (61). We note that all approaches fulfilled for moderate choices of $\nu_J$ the growth condition (74) needed for stability.

We computed the first 1000 terms in the expansion (60) and used a radius $\tau = 1.04$ with $2^{10}$ sampling points for the numerical inverse $Z$–transformation (54). For a detailed discussion of the choice of a suitable radius $\tau$ we refer the reader to [23]. In order to calculate the convolution coefficients $b_n$ (discretized

TBC of Levy) we used the MATLAB routine from [22] to compute the first 100 zeros of the Airy function.

First we examine the convolution coefficients of the two presented approaches. Fig. 1 shows a comparison of the coefficients $b_n$ from the discretized TBC (42) with the coefficients $s_J^{(n)}$ from the approximated discrete TBC. The coefficients

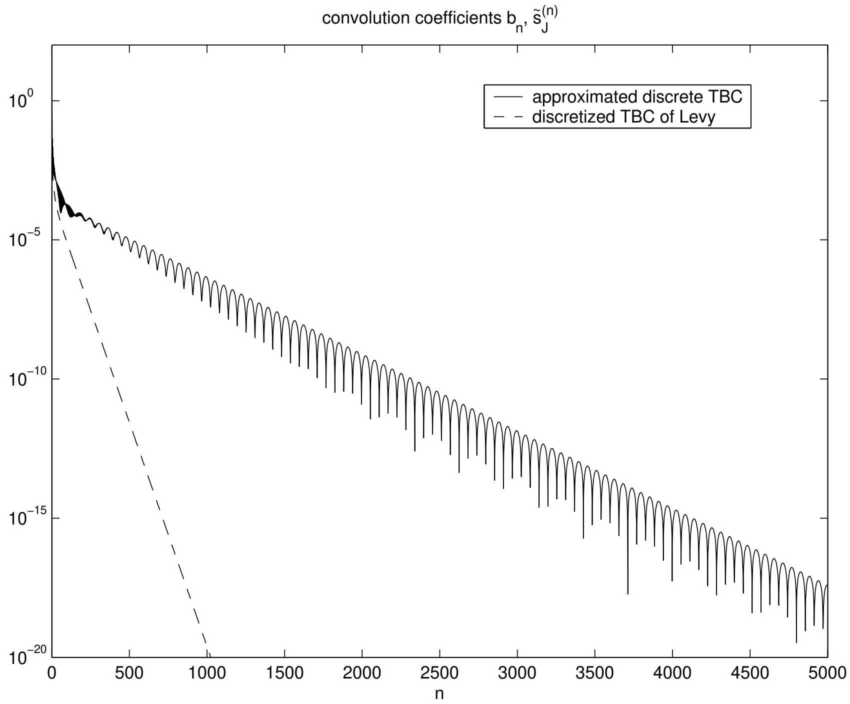


Fig. 1. Comparison of the convolution coefficients $b_n$ of the discretized TBC (42) and $\tilde{s}_J^{(n)}$ from the approximated discrete TBC (with $L = 27$).

$b_n$ decay even faster than the coefficients $s_J^{(n)}$. In Fig. 2 we plot both the exact convolution coefficients $s_J^{(n)}$ and the error $|s_J^{(n)} - \tilde{s}_J^{(n)}|$ versus $n$ for $L = 27$ (observe the different scales).

Now we investigate the stability of the approximated discrete TBC and check the growth condition (74). For $\beta = 1$ we have $\max\{\mathrm{Im}\,(\hat{g}_{\mu,J}(\beta\, e^{i\varphi})\} = 0.153$ and, with $\beta = 1.01$, we obtain $\max\{\mathrm{Im}\,(\hat{g}_{\mu,J}(\beta\, e^{i\varphi})\} = -0.002$ (see Fig. 2). This means that the $Z$–transformed kernel $\hat{g}_{\mu,J}(\beta\, e^{i\varphi})$ of the approximated discrete TBC satisfies the stability condition (74) for $\beta \geq 1.01$ (for this discretization).

In Fig. 4 and Fig. 5 we compare the transmission loss results for the discretized TBC and the approximated discrete TBC in the range from 0 to 50 km. The transmission loss curve of the solution using the approximated DTBC is indistinguishable from the one of the reference solution while the solution with the discretized TBC still deviates significantly from it (and is more oscillatory) for

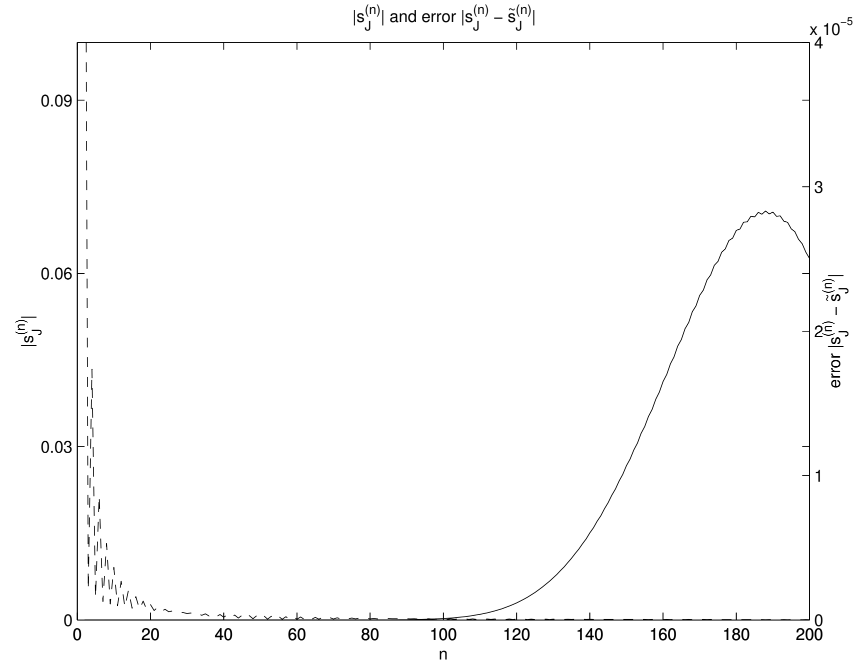


Fig. 2. Convolution coefficients $s_J^{(n)}$ (left axis, dashed line) and error $|s_J^{(n)} - \tilde{s}_J^{(n)}|$ of the convolution coefficients (right axis); $(L = 27)$.

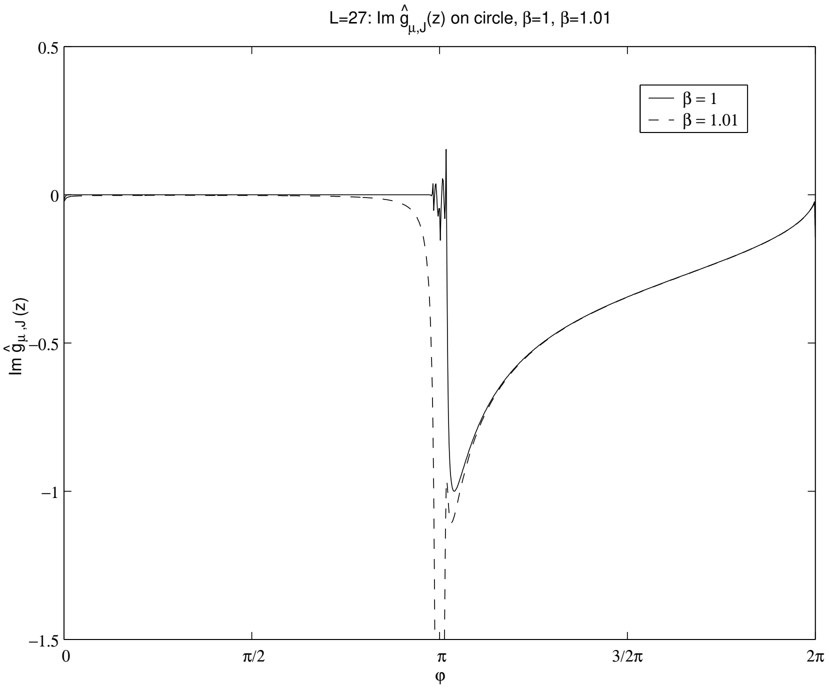


Fig. 3. Growth condition $\hat{g}_{\mu,J}(z)$, $z = \beta\, e^{i\varphi}$ $(L = 27)$.

the chosen discretization. The result in Fig. 5 does not change if we compute more zeros of the Airy function.

Evaluating the convolution appearing in the discretized TBC (42) is quite ex-

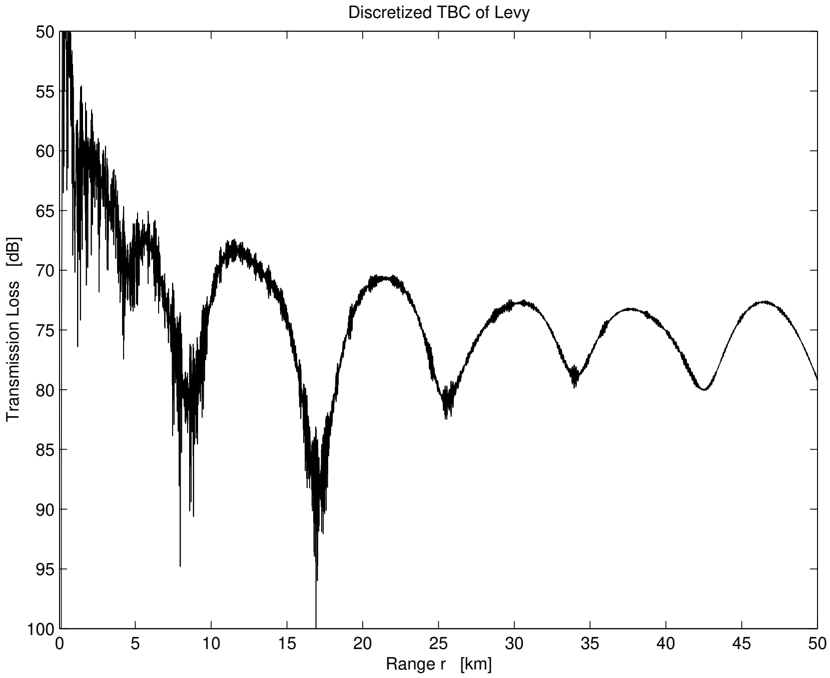


Fig. 4. Transmission loss at $z_r = 27.5\,\mathrm{m}$.

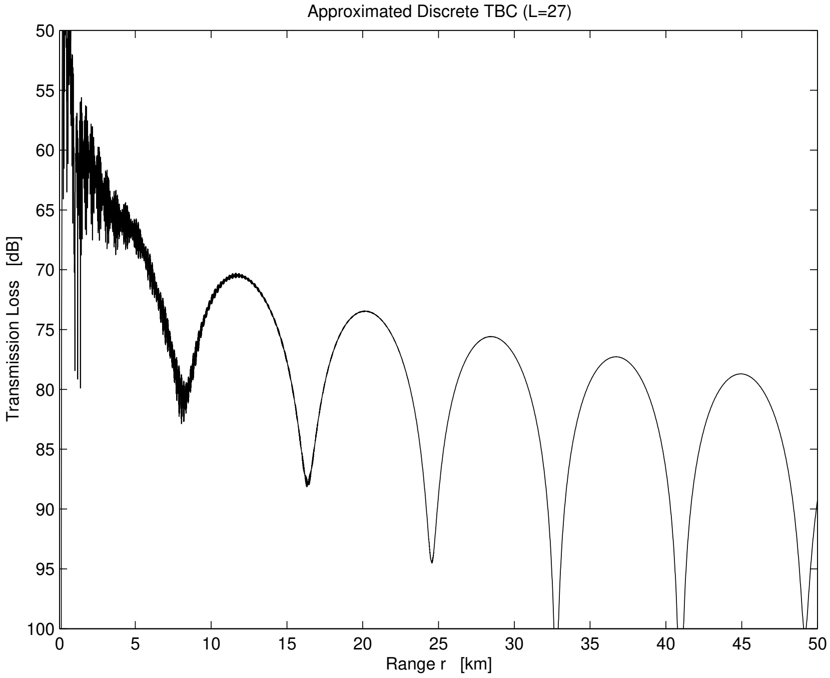


Fig. 5. Transmission loss at $z_r = 27.5\,\mathrm{m}$.

pensive for long-range calculations. Therefore we extended the range interval up to 250 km and shall now illustrate the difference in the computational effort for both approaches in Fig. 6: The computational effort for the discretized TBC is quadratic in range, since the evaluation of the boundary convolutions dominates for large ranges. On the other hand, the effort for the approximated

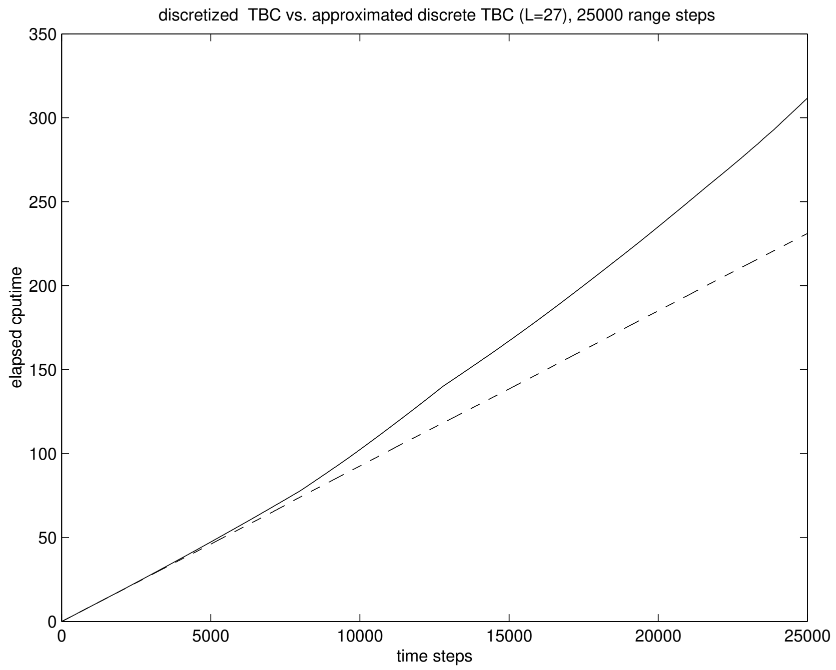


Fig. 6. Comparison of CPU times: the discretized TBC of Levy has quadratic effort (—), while the sum-of-exponential approximation to the discrete TBC has only linear effort (- - -).

discrete TBC only increases linearly. The line (- - -) does not change considerably for different values of $L$ since the evaluation of the sum-of-exponential convolutions has a negligible effort compared to solving the PDE in the interior domain.

## Conclusion

We have proposed a variety of strategies to derive an approximation to the discrete TBC for the Schrödinger equation with a linear potential term in the exterior domain. The derivation was based on the knowledge of the exact solution (including the asymptotics) to the discrete Airy equation. Our approach has two advantages over the standard approach of discretizing the continuous TBC: higher accuracy and efficiency; while discretized TBCs have usually quadratic effort, the sum-of-exponential approximation to discrete TBCs has only linear effort. Moreover, we have provided a simple criteria to check the stability of our method.

## Acknowledgement

The first author thanks Prof. A. Arnold for many helpful suggestions to this article and acknowledges support by the DFG Research Center "Mathematics for key technologies" (FZT 86) in Berlin.

## References

[1] A. Arnold, *Numerically Absorbing Boundary Conditions for Quantum Evolution Equations*, VLSI Design **6** (1998), 313–319.

[2] A. Arnold and M. Ehrhardt, *Discrete transparent boundary conditions for wide angle parabolic equations in underwater acoustics*, J. Comp. Phys. **145** (1998), 611–638.

[3] A. Arnold, M. Ehrhardt and I. Sofronov, *Approximation, stability and fast calculation of non–local boundary conditions for the Schrödinger equation*, Commun. Math. Sci. **1**, Issue 3 (2003).

[4] E.W. Barnes, *On the homogeneous linear difference equation of the second order with linear coefficients*, Messenger **34** (1904), 52–71.

[5] P.M. Batchelder, *An Introduction to Linear Difference Equations*, (Harvard University Press, Cambridge, MA, 1927).

[6] T.W. Dawson, D.J. Thomson and G.H. Brooke, *Non–local boundary conditions for acoustic PE predictions involving inhomogeneous layers*, in 3rd European Conference on Underwater Acoustics, FORTH–IACM, Heraklion, 1996, pp. 183–188.

[7] M. Ehrhardt, *Discrete Artificial Boundary Conditions*, Ph.D. Thesis, Technische Universität Berlin, 2001.

[8] M. Ehrhardt and A. Arnold, *Discrete Transparent Boundary Conditions for the Schrödinger Equation*, Riv. Mat. Univ. Parma **6** (2001), 57–108.

[9] W.G. Kelley and A.C. Peterson, *Difference equations: an introduction with applications*, (Academic Press, Boston, 1991).

[10] N.N. Lebedev, *Special Functions and their Applications*, Selected Russian Publications in the Mathematical Sciences, Prentice–Hall, 1965.

[11] D. Lee and S.T. McDaniel, *Ocean acoustic propagation by finite difference methods*, Comput. Math. Appl. **14** (1987), 305–423.

[12] W.J. Lentz, *Generating Bessel Functions in Mie Scattering Calculations Using Continued Fractions*, Appl. Opt. **15** (1976), 668–671.

[13] M.F. Levy, *Transparent Boundary Conditions for Parabolic Equation Solutions of Radiowave Propagation Problems*, IEEE Trans. Antennas Propag. **45** (1997), 66–72.

[14] M.F. Levy, *Parabolic equation models for electromagnetic wave propagation*, (IEE Electromagnetic Waves Series 45, 2000).

[15] R.E. Mickens, *Asymptotic properties of solutions to two discrete Airy equations*, J. Difference Equ. Appl. **3** (1998), 231–239.

[16] R.E. Mickens, *Asymptotic solutions to a discrete Airy equation*, J. Difference Equ. Appl. **7** (2001), 851–858.

[17] F.W.J. Olver, *Asymptotics and Special Functions*, (Academic Press, New York, 1974).

[18] F.D. Tappert, *The parabolic approximation method*, in: *Wave Propagation and Underwater Acoustics*, Lecture Notes in Physics 70, eds. J.B. Keller and J.S. Papadakis, (Springer, New York, 1977), 224–287.

[19] I.J. Thompson and A.R. Barnett, *Coulomb and Bessel Functions of Complex Arguments and Order*, J. Comp. Phys. **46** (1986), 490–509.

[20] G.N. Watson, *A treatise on the theory of Bessel functions*, 2nd ed., (Cambridge Univ. Press, Cambridge, 1966).

[21] R. Wong and H. Li, *Asymptotic expansions for second–order linear difference equations. II*, Stud. Appl. Math. **87** (1992), 289–324.

[22] S. Zhang and J. Jin, *Computation of special functions: with over 100 computer programs in FORTRAN*, John Wiley & Sons, New York, 1996). (MATLAB routines: `http://ceta.mit.edu/comp_spec_func/`)

[23] A. Zisowsky, *Discrete Transparent Boundary Conditions for Systems of Evolution Equations*, Ph.D. Thesis, Technische Universität Berlin, 2003.